Wrinkling and electroporation of giant vesicles in the gel phase†

Roland L. Knorr, Margarita Staykova, Rubèn Serral Gracià‡ and Rumiana Dimova*

Received 10th December 2009, Accepted 29th January 2010
First published as an Advance Article on the web 4th March 2010
DOI: 10.1039/b925929e

Electric pulses applied to fluid phospholipid vesicles deform them and can induce the formation of pores, which reseal after the end of the pulse. The mechanical and rheological properties of membranes in the gel phase differ significantly from those of fluid membranes, thus a difference in the vesicle behavior in electric fields is expected. However, studies addressing this problem are scarce. Here, we investigate the response of giant gel-phase vesicles to electric pulses and resolve the dynamics of deformation with microsecond resolution. We find that the critical transmembrane potential leading to poration is several times higher as compared to that of fluid membranes. In addition, the resealing of the pores is arrested. Interestingly, the vesicle shapes change from ellipsoidal to spherocylindrical during the electric pulse and the membrane becomes periodically wrinkled with ridges aligned with the field direction and wavelengths in the micrometre range. Such membrane wrinkling has not been reported previously. The corrugations comply with universal laws of wrinkling of surfaces with lengthscale dimensions from nanometres to metres.

Introduction

The behavior of cells and vesicles subjected to electric fields has been an object of extensive studies in the last couple of decades.[1–6] The phenomena of electroporation and electrofusion are of particular interest because of their vast use in cell biology and biotechnology as means for cell hybridization or for introducing molecules such as proteins, foreign genes (plasmids), antibodies, or drugs into cells. Strong electric DC-pulses of short duration induce transient pores across the cell membrane allowing the influx and efflux of molecules, or the fusion of two cells, which are in close proximity.

To understand the process of cell electroporation, a significant number of studies have been performed on model membranes. The majority of these studies have employed single-component vesicles whose lipids are in the fluid state. When subjected to weak pulses, such vesicles deform due to the electric stress imposed on the lipid bilayer. The vesicle shape change depends on the conductivity ratio between the inner and outer vesicle solution, as demonstrated on small ~100 nm vesicles[7–9] and on cell-sized giant unilamellar vesicles (GUVs).[10,11] Whereas the results for the small vesicles are based on indirect measurements, GUVs provide direct visualization of the membrane response with optical microscopy[12–16] owing to their large size.

In electric fields, the potential built across the membrane induces an effective electrical tension.[10,17] Under sufficiently strong or long pulses, the membrane of fluid phase vesicles may rupture.[10,17–19] In giant vesicles exposed to pulses in the 100 μs range, this process is accompanied by the formation of optically detectable pores with micrometre sizes.[10] In charged membranes, such pores destabilize the membrane and can lead to vesicle collapse.[20] In neutral phosphatidylcholine membranes, the pores reseal and their lifetime is typically in the range of a few tens of milliseconds.[10]

The overall behavior of the vesicles exposed to electric pulses depends strongly on the material properties of the constituting lipid bilayer. It is well known that the mechanical and rheological properties of membranes in the gel phase differ drastically from those in fluid state; for a concise comparison see ref. 15. For example, the bending stiffness and the shear surface viscosity of gel-phase membranes are orders of magnitude higher than those reported for membranes in the fluid phase,[21–24] and membranes in the gel phase are thicker.[25] Such features can be expected to leave a signature on the response of gel-phase membranes to electric fields. However, only a scarce number of studies in the literature have considered this problem. Among them, electroporation of 100 nm gel-phase vesicles was reported as transient and fully reversible with lifetime of the nanometre pores in the millisecond range.[26] On the other hand, micrometre pores induced in giant vesicles were observed as long-living.[16,27] Electric fields were also shown to affect the phase transition of certain lipids,[28] supporting an earlier theory by Sugar.[29]

A convenient lipid to investigate the response of gel-phase membranes to electric pulses is dipalmitoylphosphatidylcholine (DPPC). DPPC is the primary component of the lung surfactant[30] and is found in large amounts in the cell nuclei.[31] The main phase transition of this lipid is at 41.6 °C.[32] Thus, at room temperature DPPC membranes are in the gel phase.

We used DPPC giant vesicles to investigate the response of gel-phase membranes to DC pulses in the submillisecond range. Confocal and phase contrast microscopy in combination with fast digital imaging were employed to shed light on the behavior of gel-phase vesicles. The dynamics of deformation and poration

Max Planck Institute of Colloids and Interfaces, Science Park Golm, 14424 Potsdam, Germany. E-mail: Rumiana.Dimova@mpikg.mpg.de; Fax: +49 331 567 9615; Tel: +49 331 567 9612

† Electronic supplementary information (ESI) available: Degree of deformation of a gel-phase vesicle exposed to pulses with different field strength. See DOI: 10.1039/b925929e

‡ Present address: Culgi B.V. P.O. Box 252 2300 AG Leiden, The Netherlands.

of these vesicles differ significantly from the response of vesicles in the fluid phase. The electroporation of the gel-phase membranes appears to be an irreversible process. Surprisingly, we observe intra-pulse shape relaxation for non-porated gel-phase vesicles. This process is associated with membrane wrinkling. The vesicle surface corrugates during the pulse, forming wrinkles parallel to the field direction. This membrane behavior is analogous to wrinkling of elastic sheets.[33] Wrinkling of lipid membranes has not been previously reported.

Materials and methods

Vesicle preparation

GUVs were prepared from DPPC and palmitoyloleoylphosphatidylcholine (POPC) (Avanti Polar Lipids, Birmingham AL) using the electroformation method[34] as described in detail in ref. 10. The main phase transition of POPC occurs at −2 °C. Thus, at room temperature POPC vesicles are in the fluid phase. For fluorescence imaging, 0.1 mol% dipalmitoylphosphatidylethanolamine-Rhodamine (DPPE-Rh) from Avanti Polar Lipids was added to some of the lipid solutions.

The vesicles were grown from a lipid film deposited on the conductive side of glasses coated with indium tin oxide (ITO). The film was prepared by spreading a chloroform solution of the lipid, followed by 2 h evaporation under vacuum. Two ITO glasses were assembled to form a chamber sandwiching a 2 mm thick Teflon frame. The chamber was filled with 0.2 M sucrose solution and closed by binder clips. The conductive sides of the ITO glasses were connected to a function generator and the chamber placed in an oven at 60 °C. Alternating current at 1 V and 10 Hz was applied for 1 h, after which the field was changed to 1.5 V, 5 Hz for 2 h. Afterward, the chamber was slowly cooled down to room temperature with cooling rate lower than 0.5 °C min^{-1}. The vesicles were diluted more than 10 times in 0.2 M glucose solution to create sugar asymmetry between the vesicle interior and exterior. Because of the density difference, the vesicles settle at the bottom of the observation chamber. The difference in refractive indices of the solutions improves the vesicle contrast when observed with phase contrast microscopy. Loss of contrast in vesicles is an indication that pores, allowing the exchange of the encapsulated solution, have been or are present in the bilayer. Freshly prepared vesicles in the fluid phase exhibit good contrast, which is maintained for days after their formation. However, in suspensions of gel-phase vesicles, one often observes vesicles with poor contrast indicating compromised membrane integrity, *e.g.* presence of disclinations, holes, or grain boundaries. Such membrane defects were shown to lead to lower lysis tension as compared to membranes in the fluid phase.[35] In our experiments, we chose vesicles with good contrast, *i.e.* without or with very few and small defects in the membrane. Presumably, the number of such defects depends on the rate at which the fluid vesicles are brought to the gel phase. As pointed out above, in our procedure this rate is low.

Vesicle observation and experimental procedures

The vesicles were exposed to square-wave DC pulses with a duration of 300 μs and different field strengths. The working chamber (Eppendorf, Hamburg, Germany) consists of two parallel electrode wires, 0.2 mm in diameter and at a gap distance of 0.5 mm, fixed to a Teflon frame, and confined from above and below by two glass slides. The electrodes are situated close to the lower glass. The chamber was connected to a Multiporator (Eppendorf), which can generate DC and AC fields. Prior to the application of the DC pulses, AC field (3 V, 2 MHz) was applied for 10 s, which resulted in a negative dielectrophoretic motion of the vesicles towards the middle between the electrodes and away from the bottom glass. Such repositioning of the vesicle in the middle between the electrodes and away from the chamber bottom ensures homogeneous field distribution during the applied pulse. Note that in contrast to vesicles in the gel phase, vesicles in the fluid phase deform when subjected to AC fields[27,36] and may exhibit a membrane flow in inhomogeneous AC fields.[37]

The deformation response of the vesicles under DC pulses was observed with high temporal resolution under phase contrast by an inverted Zeiss microscope, Axiovert 135 (Jena, Germany), equipped with a 20× Ph2 objective and a fast digital camera, HG-100 K (Redlake, San Diego, CA). Image sequences were acquired either at 20 000 or 50 000 frames per second (fps). For routine observation and vesicle selection, the sample was illuminated with a halogen lamp. A mercury lamp (HBO W/2) was used only for a few seconds during recordings with the fast camera. Under this condition, sample heating from the illumination is less than 2 °C[11] and does not influence the phase state of the lipids used.

Confocal and differential interference contrast (DIC) images with higher spatial resolution were recorded using a Leica DM IRE2 SP5 system (Leica Microsystems Heidelberg GmbH, Germany), with a 40× HCX Plan APO objective (N.A. = 0.75). The fluorescently labeled vesicles were imaged with excitation at 561 nm (DPSS laser). Emission light was detected by a photomultiplier tube in the spectral range 575–650 nm. Vesicles labeled with dyes did not exhibit any difference in their dynamics of deformation and electroporation as compared to dye-free vesicles.

Image analysis

The beginning of the DC pulse, indicated as time zero in the data presented in this work, was assigned to the frame before the snapshot in which detectable vesicle deformation were observed. This procedure can lead to a certain offset error in time, which is up to 20 μs or 50 μs for acquisition speeds of 50 000 fps or 20 000 fps, respectively. The degree of the vesicle deformation was quantified by the ratio a/b, where a and b are the semi axes, along and perpendicular to the field vector, respectively; see the inset in Fig. 1. The image analysis was automated employing a home-developed program, which locates the contour of the vesicle in phase contrast micrographs with subpixel resolution.[38] Detecting the contour with high resolution is important because the deformation of vesicles in the gel phase is relatively small. The vesicle contour was expanded in Fourier series as described in ref. 38,39. The vesicle aspect ratio, a/b was extracted from the second mode in the Fourier expansion, which describes the overall elongation of the vesicle.

Results and discussion

Before we describe the results on the response of gel-phase vesicles to electric pulses, we first consider some general relations and typical timescales involved.

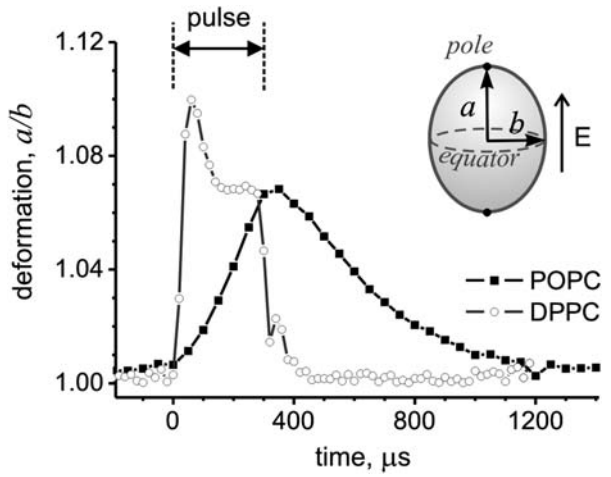

Fig. 1 Deformation response of a gel-phase DPPC vesicle with a radius of 22 μm, and a fluid-phase POPC vesicle with a radius of 20 μm to DC pulses with a duration of 300 μs. The pulse duration is indicated on the figure. The field strength of the pulses was 5 kV cm^{-1} and 0.8 kV cm^{-1} for the gel and the fluid vesicle, respectively. The measurements were performed at 22 °C. Similar data was briefly reported in ref. 27. The inset shows the semiaxes a and b of a deformed vesicle. To improve the time resolution of the measurement on the DPPC vesicle, the data is averaged over three pulses applied to the same vesicle.

Some considerations on the response of gel-phase vesicles to DC pulses

The behavior of membranes in electric fields depends on the electric properties of the surrounding media and the vesicle bilayer. Lipid membranes are impermeable to ions. Thus, in the presence of electric fields, charges accumulate on their surfaces. This process is characterized by the so called charging time τ_{charg}.[40]

$$\tau_{charg} = RC_m\,[1/\lambda_{in} + 1/(2\lambda_{ex})] \quad (1)$$

where R is the vesicle radius, λ_{in} and λ_{ex} are the conductivities of the internal and external vesicle solutions, respectively, and C_m is the membrane capacitance, expressed as:

$$C_m = \varepsilon_m\, A\, h^{-1} \quad (2)$$

Here, ε_m is the static dielectric constant of the membrane, typically assumed to be $\varepsilon_m = 2.2\ \varepsilon_0$,[41] where ε_0 is the permittivity of free space, A is unit area and h is the membrane thickness.

The membrane capacitance can be determined experimentally from patch clamp measurements,[42,43] electric current measurements on black lipid membranes,[44–46] electro-kinetic studies,[47] and impedance or permittivity measurements on vesicle suspensions.[48,49] The capacitance of lipid bilayers in the fluid phase is of the order of 0.6–1 μF cm^{-2}.[41,47] This corresponds to membrane charging time of $\tau_{charg} \cong$ 360–600 μs for vesicles of radius $R =$ 20 μm in the fluid phase and for the limiting case of salt-free solutions used here, *i.e.* for $\lambda_{in} \cong 6$ μS cm^{-1} and $\lambda_{ex} \cong 4.5$ μS cm^{-1}. This time is longer than the duration of the pulses applied in this study.

The membrane charging time is influenced by the state of the lipids. This is reflected by the temperature dependence of the membrane capacitance, which decreases below the phase transition temperature as shown for small lipid vesicles[49] and for erythrocyte membranes.[48] Several reasons for this are conceivable. First, the membrane lateral density increases by about 24% upon transition from fluid to gel phase, which is associated with straightening of the hydrophobic lipid tails leading to a larger bilayer thickness. For fluid DPPC membranes $h \cong 3.9$ nm (at 50 °C), while for DPPC membranes in the gel phase $h \cong 4.8$ nm (at 20 °C).[25] The latter increase should lead to a decrease in the membrane capacitance C_m by about 20%. Second, the tighter packing of the lipid chains in the gel phase implies fewer water molecules in the bilayer as compared to those in fluid membranes.[50] This is supported by experimental studies on the membrane permeability, which in the gel phase was measured to be 100 times lower than in the fluid phase.[51] Third, the dielectric permittivity of the membrane in gel phase is expected to be smaller than that in the fluid phase, due to the reduced rotational and translational lipid mobility.[52] Overall, the decrease in the membrane capacitance implies shorter charging time τ_{charg} for vesicles in the gel phase; see eqn (1). Taking the capacitance $C_m \cong 0.45$ μF cm^{-2},[49] one obtains the charging time $\tau_{charg} \cong 270$ μs for the gel phase membrane in salt-free solutions and a vesicle radius $R = 20$ μm as above. This time is comparable to the duration of the pulses used here. For smaller vesicles, τ_{charg} is even shorter.

Membrane charging during the electric pulse leads to re-distribution of the electric field around the vesicle and an increase in the transmembrane potential Ψ_m as a function of time t:

$$\Psi_m\,(t) = 1.5\ R\,|\cos\theta|\ E(t)\ [1 - \exp(-t/\tau_{charg})] \quad (3)$$

Here, E is the amplitude of the applied electric field, and θ is the tilt angle between the electric field and the surface normal. Note that eqn (1) and (3) are valid only for a nonconductive membrane. Pores or porous defects, which are occasionally present in gel-phase membranes as discussed in the Materials and methods section, can lead to lower transmembrane potentials.

The arising field distribution around the vesicle and the increasing field in the membrane give rise to Maxwell stresses at the membrane interfaces. These stresses can deform the vesicle. The type of deformation, prolate, oblate or spherocylindrical, depends on the conductivities of the internal and external media.[10,11] For the conditions of salt-free solutions we use here, the vesicles tend to assume prolate shapes.

For strong pulses, the high electric field in the membrane arising from its charging induces a perpendicular stress in the bilayer. Because the bilayer is almost incompressible, this stress can be associated with an increase in the membrane area (stretching). Thus, the electric field in the membrane adds an extra tension, σ_{el}, which given in terms of Ψ_m is:[17,53]

$$\sigma_{el} = \varepsilon_m\,(h/2h_c^2)\ \Psi_m^2 \quad (4)$$

where h is the total bilayer thickness as before and h_c is the thickness of the hydrophobic core of the membrane. For fluid DPPC membranes $h_c \cong 2.9$ nm (at 50 °C), while for DPPC membranes in the gel phase $h_c \cong 3.4$ nm (at 20 °C).[25]

The electroporation phenomenon, *i.e.* the membrane rupture under electric pulse exposure, occurs above some critical transmembrane potential, which for fluid membranes is around

1 V.[4,54] This threshold can also be understood in terms of critical or lysis tension, σ_{lys}, above which the membrane ruptures. For fluid membranes, σ_{lys} varies between 2 and 10 mN m^{-1} depending on the lipid.

Timescales involved in the deformation response of fluid- and gel-phase vesicles

In this section, we compare the deformation responses of fluid- and gel-phase vesicles subjected to DC pulses below the electroporation threshold. Some results from this section were briefly introduced in ref. 27. Here, we discuss in detail the various features of the deformation response of the gel-phase membranes, which compared to fluid ones is still poorly understood.

In the experiments we used POPC giant vesicles, which are in the fluid phase at room temperature, and DPPC vesicles, which are in the gel phase. We selected vesicles with similar sizes to ensure comparable charging times, which depend on the vesicle radius; see eqn (1). The vesicles were exposed to a single square-wave pulse with duration of 300 μs and pulse strength, adjusted to induce a similar degree of deformation in both vesicle types without causing poration. It must be noted that it is difficult to adjust the degree of deformation of a selected vesicle because it depends on the initial vesicle tension or excess area[10] (the excess area is defined as the excess with respect to the area of a spherical vesicles with the same volume). Both are unknown *a priori*. Gel-phase vesicles required pulses with much larger field strengths to attain an optically detectable deformation. To produce similar degree in the two vesicle types, we used pulse strengths of 0.8 and 5 kV cm^{-1} for the fluid- and gel-phase vesicles, respectively. Whereas pulses of 5 kV cm^{-1} readily cause electroporation in fluid vesicles, the membrane in the gel vesicles remains intact. For the degree of deformation attained by the gel-phase vesicles at lower field strength see Fig. S1 in the ESI.†

The dynamics of deformation response of vesicles in the fluid and gel phase differ significantly as shown in Fig. 1. The fluid vesicle gradually responds, reaching a maximal deformation at the end of the pulse. This behavior arises from the longer membrane charging time (see previous section) as compared to the pulse duration, which results in a gradual increase of the Maxwell stresses throughout the pulse. At the beginning of the pulse, the weak Maxwell surface stresses overcome the bilayer bending rigidity and membrane fluctuations are pulled out; in terms of membrane tensions, this regime is also known as entropic.[55] Later during the pulse, the stronger electric stresses cause stretching of the membrane. In both, the entropic and the stretching regime, the apparent vesicle area increases. After the end of the pulse, the fluid vesicle relaxes gradually back to a sphere, $a/b = 1$, with a characteristic decay time of 0.4 ms. This value is within the range of 0.1–0.5 ms reported for fluid, non-porated egg PC vesicles and is related to the relaxation of the bilayer stretching.[10]

Gel-phase vesicles respond faster and in a more complex fashion; see Fig. 1. The maximal deformation is already reached 60 μs after the onset of the electric field. This is not surprising bearing in mind that the field strength is six times larger than in the experiments with the fluid-phase vesicles. Furthermore, the charging time of the membrane in the gel phase is shorter than that in fluid phase; see previous section. Following eqn (3), the transmembrane potential reached in the first 60 μs in the gel-phase vesicle is 5–10 times higher than that reached in the fluid-phase vesicle. This is confirmed by the deformation of the two vesicle types in the first 60 μs in Fig. 1 when comparing $a/b - 1$, which characterizes out-of-sphere deformations.

What is intriguing in the response of the gel-phase vesicle is the decrease of the deformation already during the pulse. Measurements on different DPPC vesicles show that the decay time of this intra-pulse relaxation is in the range 30–60 μs. During the intra-pulse relaxation, a/b attains a plateau value, which can be different for every vesicle. Pulses of different field strength applied to the same vesicle change only the maximum degree of deformation, but not the value of a/b at the end of the intra-pulse relaxation; see Fig. S1 in the ESI.†

After the end of the pulse, gel-phase vesicles relax back to their initial spherical shape with a decay time of 50 ± 10 μs; see also Fig. 2. This relaxation time is 10 times shorter than that of the fluid-phase vesicles.

The intra-pulse relaxation is a very surprising phenomenon. Since the gel-phase vesicles are exposed to much stronger fields as compared to the fluid ones, one would intuitively expect membrane electroporation. However, in the example given in Fig. 1, no microscopic pores were optically detected and the vesicle contrast was preserved. This implies the absence of stable pores with sizes in the sub-micron range, which could allow the exchange of sucrose and glucose molecules between the vesicle interior and the surrounding media. We cannot exclude formation of nanometre-sized transient pores, since their presence would not change the vesicle contrast significantly.

Shape response and membrane wrinkling in gel-phase vesicles

To resolve the mechanism involved in the intra-pulse relaxation and the overall deformation response of the gel-phase vesicles,

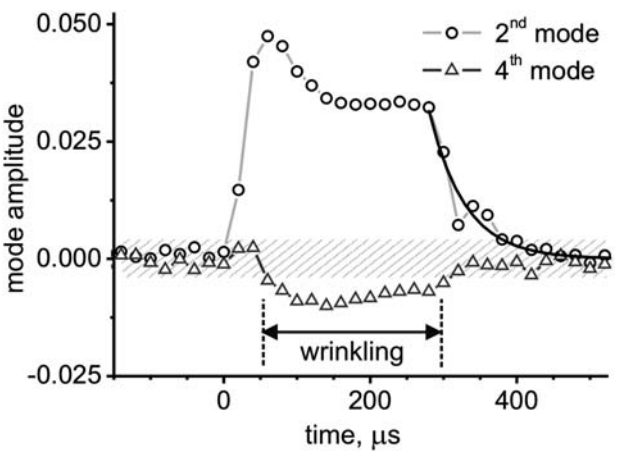

Fig. 2 Time dependence of the amplitudes of the second and fourth modes in the Fourier expansion of the shape of the DPPC vesicle from Fig. 1. The second mode shows the overall elongation of the vesicle. The black solid line is an exponential fit to the after-pulse relaxation of the second mode yielding 50 μs for the characteristic decay time of the elliptical deformation. Non-zero values of the fourth mode indicate spherocylinder-like vesicle deformation. The shaded area indicates the scattering in the data for the fourth mode measured for the vesicle in the absence of field. The deviation of the fourth mode away from this zone correlates with the period when wrinkles are observed in the vesicle.

we analyzed the recorded image sequences in detail. For this purpose, the vesicle contour was detected and expanded in Fourier series. The modes in this expansion describe the vesicle shape. We found that during the pulse the vesicle shape changes slightly from an ellipsoid to a morphology resembling a spherocylinder with a symmetry axis oriented parallel to the field direction. Non-elliptical deformations are described by higher modes in the Fourier expansion and in the case of spherocylinders, by the fourth mode. Fig. 2 shows the time dependence of both the second and the fourth modes during the pulse. The non-zero deviation of the fourth mode (shaded area in Fig. 2) reveals a non-elliptical vesicle shape transformation, which occurs around 50 μs after the beginning of the pulse and lasts until the pulse end.

A careful inspection of the vesicle images revealed another interesting phenomenon, namely the presence of stripe-like shades on the surface of the DPPC vesicle. The stripes were oriented parallel to the direction of the electric field; see the inset in Fig. 3. In microscopy images, such stripes arise from the wrinkling of the inspected surface.[56] The wavelength of the wrinkles, measured on different vesicles in our experiments, varies between 5 and 8 μm.

Similar non-elliptical deformations and wrinkled surfaces have been previously observed on polymer microcapsules in shear flow[56] but never on phospholipid membranes in the gel phase. Vesicles in the fluid phase were reported to exhibit transient wrinkling in a pulsatile elongation flow.[57] However, this behavior is of different nature, resulting from the adjustment of the negative surface tension of the membrane to alternating stress.

Wrinkling of elastic sheets has been considered theoretically.[33,58,59] According to Finken and Seifert,[59] wrinkling occurs above a certain membrane tension threshold $\sigma_w = (1/R)(K_a\kappa)^{1/2}$,

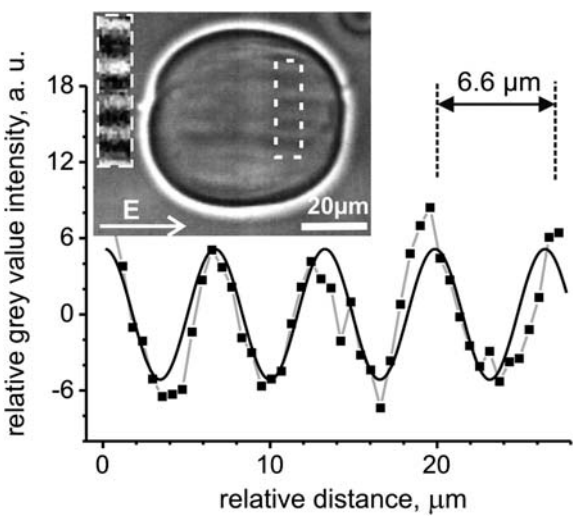

Fig. 3 Wrinkling of a DPPC vesicle during a DC pulse with field strength of 4 kV cm^{-1}, and duration of 300 μs. The inset shows a phase contrast snapshot of the vesicle 200 μs after the beginning of the pulse. The field direction is indicated with an arrow. A magnified and enhanced section of the image is given in the upper left part of the inset, showing the membrane wrinkling parallel to the electric field. The grey value intensity from such a section is plotted and fitted with a sinusoidal function (black solid curve). The corresponding wavelength of the wrinkles is about 6.6 μm as indicated on the plot.

where K_a is the stretching elasticity modulus and κ is the bending rigidity of the lipid bilayer. Membranes in the gel phase are characterized by $K_a \cong 850$ mN m^{-1},[60] and a high bending rigidity, κ in the range of 15–20 $\times 10^{-19}$ J.[15,22–24] For a vesicle with radius $R = 20$ μm, the membrane should wrinkle at tension $\sigma \geq \sigma_w \cong 6 \times 10^{-2}$ mN m^{-1}. The wrinkling wavelength λ following the estimates for flat sheets[33] is $\lambda = 2(\pi^2 L^2 \kappa/\sigma)^{1/4}$, where L is the characteristic length of the system, in our case $L \cong 2R$ and σ is the membrane tension. For $\sigma = \sigma_w$, we obtain $\lambda \cong 9$ μm. During the pulse, the membrane tension increases; see eqn (3) and (4). Thus, the wrinkles wavelength should decrease. In order of magnitude, this estimate corresponds excellently to the wavelengths we measure. This suggests that the mechanism of vesicle wrinkling is similar to that in elastic sheets subjected to stretching[33] or in microcapsules exposed to shear flow.[56]

The amplitude of the wrinkles cannot be measured experimentally. We can only speculate that it should be in the order of the wavelength of the visible light, *e.g.* around 400–600 nm, for the wrinkles to produce a pattern in the microscopy image. Theoretically, the amplitude of the wrinkles, A, can be estimated following the expression:[33] $A = (\lambda/\pi)(2\Delta/W)^{1/2}$, where Δ is the compressive transverse displacement and W is the width of the stretched sheet. For our system $\Delta/W \cong 1 - b/a$, which yields the amplitude $A \cong 0.5$–1 μm for the wrinkles shown in Fig. 3.

The deformation mechanism of the vesicles in the gel phase can be understood in view of the material properties of their membranes. As indicated above, the bending rigidity of lipid bilayers in the gel-phase is almost two orders of magnitude higher than that of fluid-phase membranes.[21–24] Thus, gel-phase vesicles deform under much higher stresses and their membranes do not fluctuate. The latter implies that the unperturbed gel-phase membranes store only limited amounts of excess area, *e.g.* in existing corrugations or out-of-plane ridges. The vesicle elongation exhibited at the beginning of the pulse probably results from straightening these corrugations and is, thus, relatively weak. In comparison, fluid vesicles exposed to strong pulses can exhibit deformations of up to 20% in a/b.[10]

Additionally, the stretching elasticity modulus of gel-phase membranes is much higher than that of fluid membranes.[60] This implies that even larger stress is required to stretch the membrane. Despite the increasing Maxwell stresses developed during the pulse, the high stretching elasticity of the gel-phase vesicle impedes further expansion of the apparent area by stretching as observed for fluid vesicles.[10] Instead of further elongating, the gel-phase vesicle prefers to wrinkle in response to the pulse.

Irreversible vesicle rupture at high field strength

We also explored the behavior of gel-phase vesicles exposed to stronger DC pulses, which induce optically detectable poration. The membrane rupture was identified by the loss of contrast of the vesicles in the phase contrast images or detected membrane integrity failure.

The example given in Fig. 4, illustrates a typical case of gel-phase vesicle rupture. The GUV is initially spherical and with good contrast, *i.e.* defect-free, as observed in phase contrast microscopy (images not shown). With the pulse, the vesicle cracks open expulsing part of the membrane away. At the same

time, the remaining vesicle shell folds in; see Fig. 4d,f. The crack-like pores in the vesicle are large and with irregular shape. They remain open within a period of more than ten minutes and the poration damage appears to be irreversible on laboratory timescale. A similar arrest was reported for mechanically induced pores in dimyristoylphosphatidylcholine membranes below the main phase transition temperature.[60] In comparison, when vesicles in the fluid phase are exposed to pulses above the poration threshold, pores with diameter of up to 5 μm can form.[10] These pores have a lifetime τ_{pore} in the order of a few tens of milliseconds. This time is defined by the pore diameter d_{pore}, the membrane surface viscosity η_d and the edge tension γ following $\tau_{pore} \sim d_{pore}\eta_d/\gamma$. The membrane viscosity diverges when the membrane crosses the main phase transition.[22] Thus, the resealing process for pores formed on membranes in the gel phase is strongly suppressed as observed in our experiments. The irregular shape of the pores in gel-phase vesicles may be further indicative for the relatively low edge tension in such membranes.

Electroporated gel-phase vesicles with sizes in the range of 100 nm were reported to reseal within milliseconds.[26,61] For pores created in such vesicles, d_{pore} should be in the nanometre range, yielding pore lifetimes which are three orders of magnitude shorter than those of the micron-size pores in giant vesicles as observed here. Furthermore, the fields applied in ref. 26,61 were in the order of 30 kV cm^{-1}. Such pulses induce Joule heating in the chamber resulting in a temperature increase of up to 15 K,[61] which can bring the membranes close to and even above the DPPC pretransition temperature of 33 °C[32] and lead to a decrease in the membrane viscosity. Finally, recent coarse-grain simulations on DPPC vesicles with similar sizes suggest that below the main phase transition temperature a fraction of the lipids in such highly curved membranes remain in the fluid phase,[62] which may further facilitate pore closure. To summarize, the response of small and giant DPPC vesicles to DC pulses differs significantly.

To determine the poration threshold of gel-phase membranes, single GUVs were subjected to pulses with a fixed duration of 300 μs and field strength above 3 kV cm^{-1}. The pulse field strength was gradually increased with an increment of 0.2 kV cm^{-1} until poration was detected from contrast loss or visible rupture. Vesicles with radii in the range between 16 and 31 μm were explored. We measured the minimum field strength at which poration occurs. Assuming that the membranes rupture at the end of the pulse, the estimated critical transmembrane potential using eqn (3) was found to be 9.8 ± 1.1 V. This value is significantly higher than the critical potential of 1 V reported for fluid membranes.[4,17,54] Thus, membranes in the gel phase can stand higher tensile stresses; for the relation between the membrane tension and the transmembrane potential see eqn (4). This is also confirmed by micropipette aspiration experiments showing that fluid-phase dimyristoylphosphatidylcholine membranes undergo lysis at tensions around 2–3 mN m^{-1}, but when in the gel phase, the membranes rupture at tensions above 15 mN m^{-1}.[63] It is important to note that the rupture process depends on the loading rate.[64–66] At high loading rates the membrane can sustain much higher tensions before it ruptures. Similar behavior was demonstrated by simulation studies, where fluid DPPC bilayers were shown to spontaneously rupture at tensions exceeding 90 mN m^{-1}.[67]

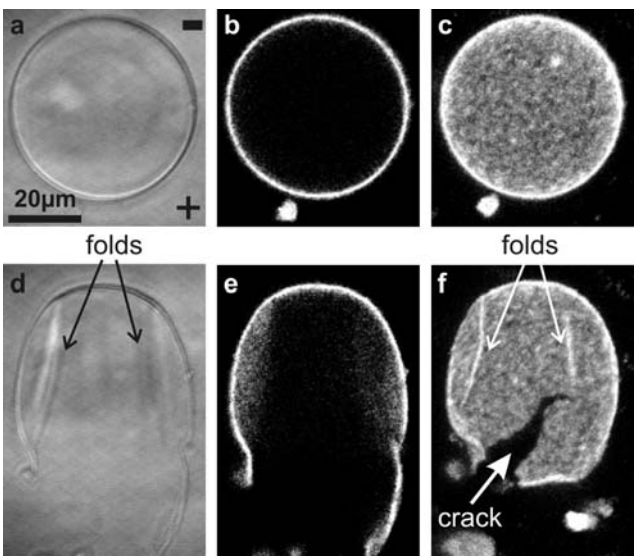

Fig. 4 Fluorescently labeled DPPC vesicle with radius 25 μm observed with bright field (a, d) and confocal microscopy (b, c, e, f). Before the pulse, the vesicle has a spherical shape: (a) DIC image, (b) confocal cross section and (c) 3D projection of the vesicle upper half. After applying a pulse with field strength of 6 kV cm^{-1} and duration of 300 μs, the vesicle cracks open and folds as indicated by the arrows in (d, f). These images were recorded a few seconds after the end of the pulse. A relatively big crack is visible in the vesicle as shown in the 3D projection of the vesicle top part (f). The electrode polarity is indicated with a plus and a minus sign in (a).

Conclusions

To the best of our knowledge, this is the first detailed study discussing the response of gel-phase giant vesicles to electric pulses. Our observations show that the behavior of gel-phase membranes differs significantly from that of fluid-phase bilayers, which have been extensively explored in the literature. The main differences are summarized as follows: (i) when exposed to pulses below the poration threshold, gel-phase vesicles deform very weakly compared to fluid-phase vesicles. Presumably, this is because of the very high bending rigidity of the former. (ii) During the pulses, gel-phase vesicles show intra-pulse relaxation associated with a shape change from an ellipsoid to a spherocylinder. The deformation is associated with wrinkling of the membrane. This is a novel observation, which has not been reported for phospholipid membranes previously. (iii) Gel-phase membranes can sustain much higher stresses and, thus, rupture at significantly higher transmembrane potentials as compared to fluid-phase bilayers. This is due to the stronger intramolecular cohesion between the lipids when in the gel phase. (iv) The poration of DPPC giant vesicles in the gel phase is irreversible on laboratory timescale.

Intuitively, one would expect that bilayers made of other fully saturated lipids behave similarly to DPPC membranes as reported here. Some differences may arise because of the lipid structure. Bilayer properties like bending rigidity are known to change as a function of chain saturation in cholesterol-doped membranes.[38,68,69] This suggests differences in the intermolecular

interactions as a function of the lipid architecture. Whether this would have an effect on the electro-deformation and -poration of vesicles remains to be clarified.

Acknowledgements

We acknowledge P. Vlahovska, U. Seifert and V. Knecht for the helpful and stimulating discussions.

Notes and references

1 E. Neumann, A. E. Sowers and C. Jordan, *Electroporation and electrofusion in cell biology*, Plenum, New York, 1989.
2 D. C. Chang, B. M. Chassy, J. A. Saunders and A. E. Sowers, *Guide to electroporation and electrofusion*, Academic Press, San Diego, 1992.
3 U. Zimmermann and G. A. Neil, *Electromanipulation of cells*, CRC Press, Boca Raton, 1996.
4 J. C. Weaver and Y. A. Chizmadzhev, *Bioelectrochem. Bioenerg.*, 1996, **41**, 135–160.
5 J. Teissie, M. Golzio and M. P. Rols, *Biochim. Biophys. Acta, Gen. Subj.*, 2005, **1724**, 270–280.
6 R. Dimova, in *Advanced electroporation techniques in biology and medicine*, ed. A. G. Pakhomov, D. Miklavcic and M. S. Markov, CRC Press, Boca Raton, Chapter 5, in press.
7 E. Neumann, K. Toensing, S. Kakorin, P. Budde and J. Frey, *Biophys. J.*, 1998, **74**, 98–108.
8 T. Griese, S. Kakorin and E. Neumann, *Phys. Chem. Chem. Phys.*, 2002, **4**, 1217–1227.
9 S. Kakorin and E. Neumann, *Colloids Surf., A*, 2002, **209**, 147–165.
10 K. A. Riske and R. Dimova, *Biophys. J.*, 2005, **88**, 1143–1155.
11 K. A. Riske and R. Dimova, *Biophys. J.*, 2006, **91**, 1778–1786.
12 W. Harbich and W. Helfrich, *Z. Naturforsch., A: Phys. Sci.*, 1979, **34**, 1063–1065.
13 D. V. Zhelev and D. Needham, *Biochim. Biophys. Acta, Biomembr.*, 1993, **1147**, 89–104.
14 E. Tekle, R. D. Astumian, W. A. Friauf and P. B. Chock, *Biophys. J.*, 2001, **81**, 960–968.
15 R. Dimova, S. Aranda, N. Bezlyepkina, V. Nikolov, K. A. Riske and R. Lipowsky, *J. Phys.: Condens. Matter*, 2006, **18**, S1151–S1176.
16 R. Dimova, K. A. Riske, S. Aranda, N. Bezlyepkina, R. L. Knorr and R. Lipowsky, *Soft Matter*, 2007, **3**, 817–827.
17 D. Needham and R. M. Hochmuth, *Biophys. J.*, 1989, **55**, 1001–1009.
18 K. T. Powell and J. C. Weaver, *Bioelectrochem. Bioenerg.*, 1986, **15**, 211–227.
19 T. Portet, F. C. I. Febrer, J. M. Escoffre, C. Favard, M. P. Rols and D. S. Dean, *Biophys. J.*, 2009, **96**, 4109–4121.
20 K. A. Riske, R. L. Knorr and R. Dimova, *Soft Matter*, 2009, **5**, 1983–1986.
21 T. Heimburg, *Biochim. Biophys. Acta, Biomembr.*, 1998, **1415**, 147–162.
22 R. Dimova, B. Pouligny and C. Dietrich, *Biophys. J.*, 2000, **79**, 340–356.
23 C. H. Lee, W. C. Lin and J. P. Wang, *Phys. Rev. E: Stat., Nonlinear, Soft Matter Phys.*, 2001, **64**, 020901.
24 K. R. Mecke, T. Charitat and F. Graner, *Langmuir*, 2003, **19**, 2080–2087.
25 J. F. Nagle and S. Tristram-Nagle, *Biochim. Biophys. Acta*, 2000, **1469**, 159–195.
26 J. Teissie and T. Y. Tsong, *Biochemistry*, 1981, **20**, 1548–1554.
27 R. Dimova, N. Bezlyepkina, M. D. Jordo, R. L. Knorr, K. A. Riske, M. Staykova, P. M. Vlahovska, T. Yamamoto, P. Yang and R. Lipowsky, *Soft Matter*, 2009, **5**, 3201–3212.
28 M. Thurk and D. Porschke, *Biochim. Biophys. Acta, Biomembr.*, 1991, **1067**, 153–158.
29 I. P. Sugar, *Biochim. Biophys. Acta, Biomembr.*, 1979, **556**, 72–85.
30 J. Goerke, *Biochim. Biophys. Acta*, 1998, **1408**, 79–89.
31 A. N. Hunt, G. T. Clark, G. S. Attard and A. D. Postle, *J. Biol. Chem.*, 2001, **276**, 8492–8499.
32 C. B. Fox, R. H. Uibel and J. M. Harris, *J. Phys. Chem. B*, 2007, **111**, 11428–11436.
33 E. Cerda and L. Mahadevan, *Phys. Rev. Lett.*, 2003, **90**, 074302.
34 M. I. Angelova and D. S. Dimitrov, *Faraday Discuss. Chem. Soc.*, 1986, **81**, 303–311.
35 H. V. Ly and M. L. Longo, *Macromol. Symp.*, 2005, **219**, 97–122.
36 S. Aranda, K. A. Riske, R. Lipowsky and R. Dimova, *Biophys. J.*, 2008, **95**, L19–L21.
37 M. Staykova, R. Lipowsky and R. Dimova, *Soft Matter*, 2008, **4**, 2168–2171.
38 R. S. Gracia, N. Bezlyepkina, R. L. Knorr, R. Lipowsky and R. Dimova, *Soft Matter*, in press, DOI: 10.1039/B920629A.
39 J. Pecreaux, H. G. Dobereiner, J. Prost, J. F. Joanny and P. Bassereau, *Eur. Phys. J. E*, 2004, **13**, 277–290.
40 K. Kinosita, I. Ashikawa, N. Saita, H. Yoshimura, H. Itoh, K. Nagayama and A. Ikegami, *Biophys. J.*, 1988, **53**, 1015–1019.
41 R. Pethig and D. B. Kell, *Phys. Med. Biol.*, 1987, **32**, 933–970.
42 E. Neher and A. Marty, *Proc. Natl. Acad. Sci. U. S. A.*, 1982, **79**, 6712–6716.
43 N. Fidler and J. M. Fernandez, *Biophys. J.*, 1989, **56**, 1153–1162.
44 R. Benz and K. Janko, *Biochim. Biophys. Acta, Biomembr.*, 1976, **455**, 721–738.
45 S. Ohki, *Biophys. J.*, 1969, **9**, 1195–1205.
46 A. G. Petrov and V. S. Sokolov, *Eur. Biophys. J.*, 1986, **13**, 139–155.
47 K. L. Chan, P. R. C. Gascoyne, F. F. Becker and R. Pethig, *Biochim. Biophys. Acta, Lipids Lipid Metab.*, 1997, **1349**, 182–196.
48 J. Z. Bao, C. C. Davis and R. E. Schmukler, *Biophys. J.*, 1992, **61**, 1427–1434.
49 M. A. Stuchly, S. S. Stuchly, R. P. Liburdy and D. A. Rousseau, *Phys. Med. Biol.*, 1988, **33**, 1309–1324.
50 K. Tu, D. J. Tobias, J. K. Blasie and M. L. Klein, *Biophys. J.*, 1996, **70**, 595–608.
51 A. Carruthers and D. L. Melchior, *Biochemistry*, 1983, **22**, 5797–5807.
52 D. B. Kell and C. M. Harris, *Eur. Biophys. J.*, 1985, **12**, 181–197.
53 I. G. Abidor, V. B. Arakelyan, L. V. Chernomordik, Y. A. Chizmadzhev, V. F. Pastushenko and M. R. Tarasevich, *Bioelectrochem. Bioenerg.*, 1979, **6**, 37–52.
54 T. Y. Tsong, *Biophys. J.*, 1991, **60**, 297–306.
55 E. Evans and W. Rawicz, *Phys. Rev. Lett.*, 1990, **64**, 2094–2097.
56 A. Walter, H. Rehage and H. Leonhard, *Colloids Surf., A*, 2001, **183–185**, 123–132.
57 V. Kantsler, E. Segre and V. Steinberg, *Phys. Rev. Lett.*, 2007, **99**, 178102.
58 E. Cerda, K. Ravi-Chandar and L. Mahadevan, *Nature*, 2002, **419**, 579–580.
59 R. Finken and U. Seifert, *J. Phys.: Condens. Matter*, 2006, **18**, L185–L191.
60 D. Needham and E. Evans, *Biochemistry*, 1988, **27**, 8261–8269.
61 E. M. Elmashak and T. Y. Tsong, *Biochemistry*, 1985, **24**, 2884–2888.
62 H. J. Risselada and S. J. Marrink, *Soft Matter*, 2009, **5**, 4531–4541.
63 E. Evans and D. Needham, *J. Phys. Chem.*, 1987, **91**, 4219–4228.
64 E. Evans, V. Heinrich, F. Ludwig and W. Rawicz, *Biophys. J.*, 2003, **85**, 2342–2350.
65 E. Evans and V. Heinrich, *C. R. Phys.*, 2003, **4**, 265–274.
66 P. A. Boucher, B. Joos, M. J. Zuckermann and L. Fournier, *Biophys. J.*, 2007, **92**, 4344–4355.
67 H. Leontiadou, A. E. Mark and S. J. Marrink, *Biophys. J.*, 2004, **86**, 2156–2164.
68 J. Pan, S. Tristram-Nagle, N. Kucerka and J. F. Nagle, *Biophys. J.*, 2008, **94**, 117–124.
69 J. J. Pan, T. T. Mills, S. Tristram-Nagle and J. F. Nagle, *Phys. Rev. Lett.*, 2008, **100**, 198103.

Wrinkling and electroporation of giant vesicles in the gel phase

Roland L. Knorr, Margarita Staykova, Rubèn Serral Gracià and Rumiana Dimova*

Max Planck Institute of Colloids and Interfaces, Science Park Golm, 14424 Potsdam, Germany
** Address correspondence to Rumiana.Dimova@mpikg.mpg.de; Fax: +49 331 567 9615; Tel: +49 331 567 9612*

Supplementary Information

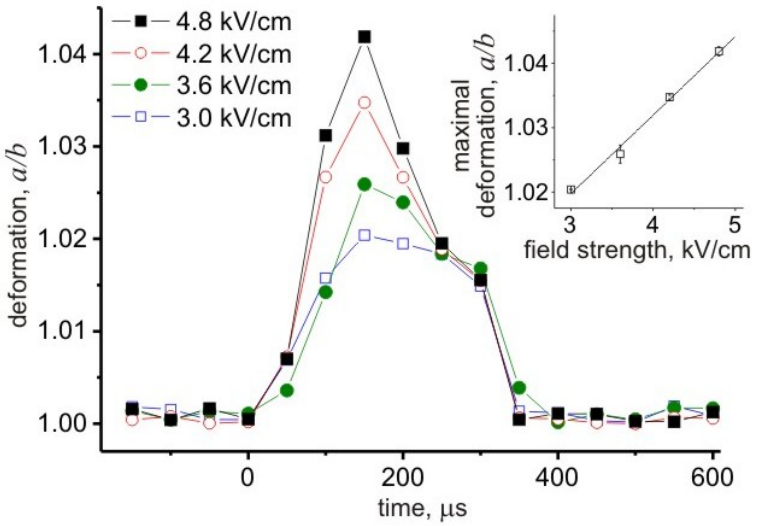

Figure S1. Deformation response of a giant DPPC vesicle with radius of 29 µm exposed to pulses with duration of 300 µs and increasing field strength as indicated in the legend. No poration was observed. The vesicle was recorded at 20 000 fps. After reaching the maximal deformation at 150 µs, intra-pulse relaxation is observed; see the main text for details. The degree of deformation at the end of the intra-pulse relaxation is similar for all pulses. The maximal degree of deformation increases linearly with the field strength of the pulse as shown in the inset. All data are averaged over three identical pulses.